16. Aksenov A. A., Mansurov Yu. N., Ivanov D. O., Reva V. P., Kadyrova D. S., Shuvatkin R. K., Kim E. D. Mechanical Alloying of Secondary Raw Material for Foam Aluminum Production. *Metallurgist*. 2017. Vol. 61, Iss. 5–6. pp 475–484.

17. Thermo-Calc Software. Available at:www.thermocalc.com (accessed: 23.11.2018).

18. Khansen M., Anderko K. The structures of binary alloys. Vol. 1. Translated from English. Moscow : Metallurgizdat, 1962. 608 p.

19. Mondolfo L. F. Aluminum Alloys: Structure and Properties. Butterworths. London/Boston : Butterworth & Co Publishers Ltd., 1976. 971 p.

20. Moore D. M., Morris L. R. Superplastic aluminium alloy products and method of preparation. Patent UK, No. 1580281. 1978.

21. Moore D. M., Morris L. R. A new superplastic aluminum sheet alloy. *Materials Science and Engineering*. 1980. Vol. 43, No. 1. pp. 85–92.

22. Ilenko V. M. Superplasticity of eutectic alloys on the basis of aluminum-calcium system and development of materials for superplastic forming: Dissertation ... of Candidate of Engineering Sciences. Moscow : MISiS, 1985. 264 p.

23. Swaminathan K., Padmanabhan K. A. Tensile flow and fracture behaviour of a superplastic Al–Ca–Zn alloy. *J. Mater. Sci*. 1990. Vol. 25, No. 11. pp. 4579–4586.

24. Perez-Prado M. T., Cristina M. C., Ruano O. A., Gonza G. Microstructural evolution of annealed Al–5%Ca–5% Zn sheet alloy. *J. Mater. Sci*. 1997. Vol. 32. pp. 1313–1318.

25. Kono N., Tsuchida Y., Muromachi S., Watanabe H. Study of the AlCaZn ternary phase diagram. *Light Metals*. 1985. Vol. 35. pp. 574–580.

26. Belov N. A., Naumova E. A., Akopyan T. K. Eutectic alloys based on aluminum: new alloying systems. Moscow : "Ore and Metals" Publishing House, 2016. 256 p.

27. Rudnev V. S., Yarovaya T. P., Nedozorov P. M., Mansurov Y. N. Wear-resistant oxide coatings on aluminum alloy formed in borate and silicate aqueous electrolytes by plasma electrolytic oxidation. *Protection of Metals and Physical Chemistry of Surfaces*. 2017. Vol. 53, Iss. 3. pp. 466–474.

28. Rudnev V. S., Nedozorov P. M., Yarovaya T. P., Mansurov Yu. N. Local plasma and electrochemical oxygenating on the example of AMg5 (AMr5) alloy. *Tsvetnye Metally*. 2017. No. 1. pp. 59–64. DOI: 10.17580/tsm.2017.01.10 NFM

Powder technology for manufacturing compact blanks of Ti – Nb – Ta, Ti – Nb – Zr alloys

A. V. Kasimtsev, *Director*[1], *e-mail: metsintez@yandex.ru*
S. N. Yudin, *Head of the Process Office*[1], *e-mail: Sergey-USN@mail.ru*
S. S. Volodko, *Post-Graduate Student, Chair of Physics of Metals and Science of Materials*[2], *e-mail: volodko.sv@yandex.ru*
A. V. Alpatov, *Senior Research Officer, Laboratory of Material Diagnostics (No. 17)*[3], *e-mail: alpat72@mail.ru*

[1] *Metsintez LLC, Tula, Russia.*
[2] *Tula State University, Tula, Russia.*
[3] *A. A. Baikov Institute of Metallurgy and Material Science of the Russian Academy of Sciences, Moscow, Russia.*

Presented in the paper are the results of investigating the consolidation process (compacting, sintering, hot isostatic pressing – HIP) of calcium hydride powder of low modulus Ti – Nb alloys doped by tantalum: Ti – 30.1 wt.% Nb – 17.4 wt.% Ta (Ti – 22 at.% Nb – 6 at.% Ta), zirconium: Ti – 33.2 wt.% Nb – 8.6 wt.% Zr (Ti – 22 at.% Nb – 6 at.% Zr) and estimating their mechanical properties. It is shown that metal powders are notable for good compactability on both single-action compacting and isostatic forming. Cold isostatic forming under pressure of 200 MPa permits to obtain briquettes with relative density of 65–68%. Sintering the briquettes at a temperature of 1873 K provides blank formation with porosity of 16 and 8% for Ti – 30.1Nb – 17.4Ta, Ti – 33.2Nb – 8.6Zr (wt.%) alloys, respectively. Sintering in vacuum of 1.33 Pa leads to formation of a gas-filled layer with heightened microhardness to a depth of 8 mm. Sintering in vacuum of $1.33 \cdot 10^{-2}$ Pa allows to avoid this phenomenon. Hot isostatic pressing of the sintered blanks at a temperature of 1193 K and pressure of 150 MPa guarantees obtaining practically porousless material (1% of pores). It is determined that Ti – 30.1Nb – 17.4Ta, Ti – 33.2Nb – 8.6Zr (wt.%) are characterized after sintering by the following values of the yield stress and the Young's modulus: $\sigma_{0.2} = 444 \pm 7$ MPa, $E = 57 \pm 5$ GPa and $\sigma_{0.2} = 570 \pm 29$ MPa, $E = 62 \pm 5$ GPa, respectively. After HIP: $\sigma_{0.2} = 791 \pm 16$ MPa, $E = 87 \pm 4$ GPa and $\sigma_{0.2} = 750 \pm 50$ MPa, E = 81 ± 1 GPa, respectively.

Key words: titanium alloys, low modulus alloys, compacting, sintering, hot isostatic pressing, porosity, yield stress, the Young's modulus.

DOI: 10.17580/nfm.2018.02.06

Introduction

Titanium alloys have widespread application in medicine owing to combination of high corrosion stability and strength with low modulus of elasticity [1–2]. Among them, the Ti – Nb alloys doped by Zr, Ta occupy a very special place [3–4]. The listed alloying additions (Zr, Nb, Ta) are remarkable for good biocompatibility and survival in human organism [5–7]. Theoretical calculations based on first principles [8–9] show that as a Nb and Ta fraction in titanium grows, its Young's modulus drops and reaches the minimal value at Nb or Ta concentration of about 25 at.%. Zirconium makes slight impact upon the Young's modulus of titanium [9]. It is known [10], that niobium is a β-stabilizer for titanium, and the single-phase β-state only is fixed after hardening the Ti – Nb alloy at niobium concentration above 24 at.%. The Ti – Nb system alloying by the third component (Ta, Zr) heighten the β-phase stability and rather broadens domain of existence [11–14].

The way of manufacturing alloys of Ti – Nb – Ta, Ti – Nb – Zr systems of greatest abundance is vacuum arc or induction smelting of initial furnace charge components followed by ingot crystallization [14–17]. High refractoriness and great difference between melting temperatures of the components seriously complicates smelting process. Liquating effects occurring during the ingot crystallization impede obtaining goods of high quality. To increase the chemical composition homogeneity of Ti – Nb – Ta and Ti – Nb – Zr alloys it is required to lessen mass of the casting and to implement several (up to 10) remeltings followed by homogenizing annealing.

An alternative way of manufacturing the alloys of Ti – Nb – Ta, Ti – Nb – Zr systems is powder metallurgy, which allows obtaining goods with required geometry and porosity by consolidation of powdered materials. In the present paper, there is suggested a method of obtaining the compact blanks based on calcium hydride synthesis of the powder of corresponding composition with its following consolidation by the methods of compacting, vacuum sintering and hot isostatic pressing.

Hence, the aim of the presented paper is to develop optimal parameters for consolidation of calcium hydride Ti – Nb – Ta, Ti – Nb – Zr powders in order to form compact blanks of alloys with controlled porosity level and to estimate their mechanical and elastic properties.

Materials and research procedure

The TiNbTa and TiNbZr powders (Table 1), synthesized by a calcium hydride method, have served as initial material for obtaining compact blanks. The exhaustive data on physical and chemical as well as the process features of the powdered TiNbTa and TiNbZr alloys are described in [18], according to which the alloys have had a β-Ti structure with the lattice period of 0.3314 and 0.3311 nm respectively.

The powders forming was carried out according to two schemes: cold isostatic forming (CIF) on a CIP 62330 hydrostat from AvureTechnologies (USA); single-action compacting on a P6320B (П6320Б) hydraulic press. Sintering has been implemented in a CShVE-1.25/25-I2 (СШВЭ-1,25/25-И2) vacuum electric pit-type heating furnace. The sintering temperature has varied from 1873 до 1973 K and the sintering time has varied from 0.5 to 3 h, as the investigation purpose has required. The heating rate was ~10 K/min. Vacuum has amounted to about 1.33 or $1.33 \cdot 10^{-2}$ Pa. The accuracy of temperature control during sintering: ±5 K. Cooling of the specimens after sintering has been fulfilled with the furnace. Hot isostatic pressing (HIP) has been implemented on an ABRA HIPP 20-70/200/2000 hot isostatic pressing apparatus (Switzerland) under the following operation conditions: temperature of 1193±10 K, gas (argon) pressure 150 MPa, holding time of 2 hours. Before HIP, the blanks have been placed into the steel capsules and hermetically soldered up. Cooling the capsules after HIP has been carried out in a chamber of hot isostatic press.

Survey of diffraction spectra has been implemented on DRON-3 (ДРОН-3) automated diffractometer with the use of homogeneous CuK_α radiation. Phase composition and lattice spacing of phases have been determined with the software package [19]. Content of gas-forming impurities has been determined on LECO (USA) equipment: a TC-600 oxygen and nitrogen analyzer; a RHEN602 hydrogen analyzer. The structure has been studied on a ZEISS Axio Observer.D1m light microscope.

To determine density of compact specimens the hydrostatic weighing method has been applied according to State Standart 18898-89 (with precision of measurements ±2%). The microhardness has been measured on a PMT-3 (ПМТ-3) apparatus with the load of 1 H (100 g) and holding time of 30 s. Mechanical properties in case of uniaxial tension have been determined on a Zwick Z250

Table 1
Chemical composition of TiNbTa and TiNbZr powders [18]

Alloy	Main elements				Impurities						
	wt.%				wt.%						
	Ti	Nb	Zr	Ta	Fe	Ni	Ca	O	N	C	H
TiNbTa	main	30.1	–	17.4	0.085	0.3	0.43	0.12	0.12	0.099	0.41
TiNbZr	main	33.2	8.67	–	0.07	0.2	0.40	0.19	0.072	0.081	0.20

testing machine at room temperature. The deformation at strain rate was equal to 10^{-3} s^{-1}. As a result there has been taken an average value, obtained in three sequential tests. Cylindrical specimens for strain have been prepared according to State Standart 1497–84. Deformation at strain has been controlled by contact extensometer.

Results and discussion

Forming is the first stage of obtaining the compact specimens. The experiments on pressing the TiNbTa and TiNbZr powders by the methods of single-action compacting and cold isostatic forming have been implemented (Fig. 1).

For lack in the scientific and technical literature of data on densities of TiNbTa, TiNbZr alloys with the component concentration similar to present alloys (Table 1), calculation of their theoretical density has been fulfilled. For that purpose, we have proceeded from the assumption that volume of the alloy equals to the sum of volumes of its component parts ($V_{al} = V_{Ti} + V_{Nb} + V_{Ta/Zr}$), the mass of alloy is also defined by the sum of masses of the component parts ($m_{al} = m_{Ti} + m_{Nb} + m_{Ta/Zr}$). Then the density of TiNbTa and TiNbZr alloys, consisting of three components may be estimated by the following formula:

$$\frac{1}{\rho_{al}} = \frac{X_{Ti}}{\rho_{Ti}} + \frac{X_{Nb}}{\rho_{Nb}} + \frac{X_{Ta/Zr}}{\rho_{Ta/Zr}}, \quad (1)$$

where ρ_{al} is a theoretical density of alloy, g/cm^3; ρ_{Ti}, ρ_{Nb} and $\rho_{Ta/Zr}$ are correspondingly densities of titanium, niobium and tantalum or zirconium subject to an alloy, g/cm^3; X_{Ti}, X_{Nb} and $X_{Ta/Zr}$ are correspondingly mass fractions of titanium, niobium and tantalum or zirconium in alloy, relative units. Concentrations (wt.%) of main elements are listed in Table 1.

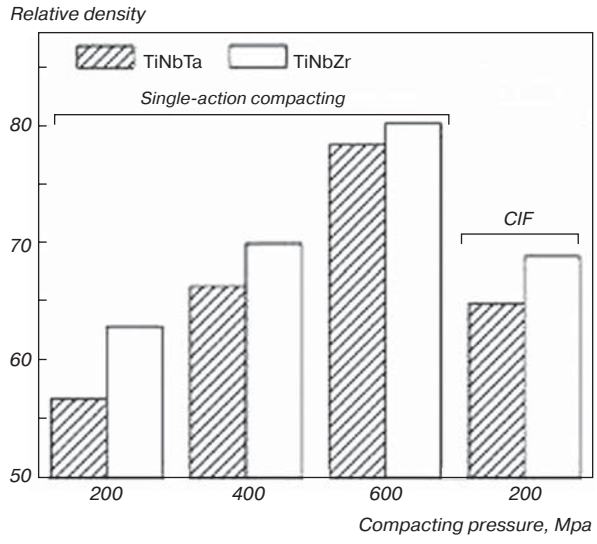

Fig. 1. The compacting scheme and pressure influence on relative density of extruded briquettes of TiNbTa (ρ_{theor} = 6.17 g/cm^3) and TiNbZr (ρ_{theor} = 5.52 g/cm^3) alloys

Thus, calculation ns according to the formula (1) show that densities of TiNbTa and TiNbZr alloy should be equal to 6.17 g/cm^3 and 5.52 g/cm^3, respectively.

The density rises as pressure of single-action compacting increases (Fig. 1). The process of pressing under the load of 200 MPa allows to produce fragile briquettes, which are failing at slight pressure. The pressure increasing up to 400 MPa promotes the strength growth of briquettes, the edges of which cease to peel off. The isostatic forming with a uniform pressing transmission to the powder allows to obtain strong compressing even at pressure of 200 MPa. Respectively, the optimal pressing scheme is cold isostatic forming.

Accurate information regarding melting temperature of the alloys under investigation (Table 1) is lacking in the scientific and technical literature. It is known [20] that the closer to the melting-point of the main component sintering of titanium alloys is conducting, the greater density is reached by the material. This fact is in complete concordance with the general theory of solid-phase sintering of metal powders [21]. Primordial attempts to estimate Tmelt of alloys in the powder state by means of differential scanning calorimetry have not yielded trustworthy results. According to the data of [22–23], it may be assumed that the optimal range of sintering temperatures for alloys from Table 1 falls between 1873–1973 K. A series of sintering has been fulfilled in order to estimate this optimal temperature: compacts in the form of cylindrical specimens with weight of about 3 g have been treated by vacuum ($1.33 \cdot 10^{-2}$ Pa) sintering at temperatures of 1873, 1923 and 1973 K during 30 min. The sintering has been implemented on molybdenum substrate. The results are shown in Fig. 2.

Heating the compact of TiNbZr powder (Fig. 2, *a*) up to the sintering temperature 1973 K (with an error in temperature estimate of ± 5 K) leads to its complete melting (Fig. 2, *d*). At a temperature of 1923 K the material (TiNbZr) is noticeably fused (Fig. 2, *b*). The TiNbTa alloy is of evidently greater refractoriness. At the sintering temperature 1973 K it is just slightly fused (Fig. 2, *e*), keeping its cylindrical shape, while at 1923 K is not melted at all (Fig. 2, *c*). After sintering the TiNbTa and TiNbZr compacts at 1873 K, compact material is forming without traces of burn-off. Hence, the sintering temperature of 1873 K is optimal with relation to process security and avoidance of possible melting of specimens.

Within the framework of this paper an influence of pressure of residual gases in the furnace chamber on quality of resulting product has been also studied. For that, sintering of compacts (∅40 mm) has been implemented at 1873 K under vacuum of 1.33 and $1.33 \cdot 10^{-2}$ Pa. It is known [24–25], that thermal treatment of titanium alloys in a medium containing oxygen and/or nitrogen leads to diffusion of interstitial impurity deep into metal with

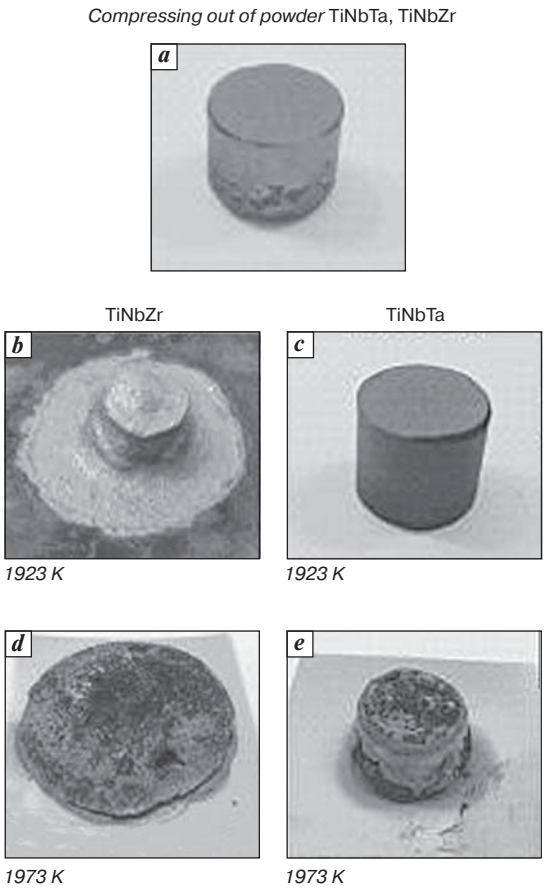

Fig. 2. An outward appearance of TiNbTa and specimens after high-temperature sintering at 1923 and 1973 K (explanations may be found in the text)

formation of a gas-filled layer. As a result, an increase of the titanium alloy microhardness will be observed, and since oxygen and nitrogen are the α-stabilizers of titanium, the near-surface microstructure modification accompanied by an α-phase appearance, has as a rule needle-shaped structure. Such a situation is possible on sintering titanium alloys in low vacuum.

In Fig. 3 is demonstrated the microstructure of TiNbTa and TiNbZr alloys after sintering under low and high vacuum conditions. The specimens sintered in low vacuum (Fig. 3, *a*, *b*) have typical alfa structure.

In order to estimate the depth of alfa layer, measurement of microhardness of the specimens has been implemented from the surface deep down. The measurement step was 100–150 μm; 5–7 pricks have been made on each step. The results are illustrated in Fig. 4.

It is evident, that microhardness of the surface layer essentially increases after sintering the alloys under low vacuum conditions (1.33 Pa) and lessens on moving away from the surface (Fig. 4, *a*, *b*). At a distance of 6-8 mm from the surface the microhardness arrives at a constant level of about 200 MPa. Sintering in vacuum of $1.33 \cdot 10^{-2}$ Pa permits to avoid the surface gasing (Fig. 4, *c*, *d*) and to obtain uniform grain structure (Fig. 3, *c*, *d*).

Table 2 contains the results of estimating the oxygen, nitrogen and hydrogen content in the surface layer (sampling has been carried out at a distance of 2 mm from the edge) and in the center (sampling has been carried out at a distance of 15 mm from the surface) of the specimens under investigation. As it is seen from Table 2, the surface after sintering under low vacuum (1.33 Pa) is characterized by very high concentration of oxygen and slightly heightened content of nitrogen. When pressure of residual gases in the furnace chamber comes to ~$1.33 \cdot 10^{-2}$ Pa, content of O and N on the surface and in the center does not differ significantly. Presence of vacuum, even low, effectively affects the hydrogen decrease relative to the powered state (Table 1).

Phase analysis has shown that in the surface layers of compact alloys sintered under low vacuum conditions (1.33 Pa) presented are titanium oxide (TiO) and nitride (TiN) along with the Ti-based β-hard solution, which is not present in case of the sintering in high vacuum ($1.33 \cdot 10^{-2}$ Pa). In all cases, central layers of the specimens were represented by β-Ti only. As a result, we observe a dependence of the microhardness value upon the distance from the surface of a specimen after sintering in low vacuum and stable microhardness values after sintering in high vacuum (Fig. 4). Thus, the optimal condition for the TiNbTa and TiNbZr alloys sintering is providing with the pressure of residual gases in the furnace no greater than $1.33 \cdot 10^{-2}$ Pa.

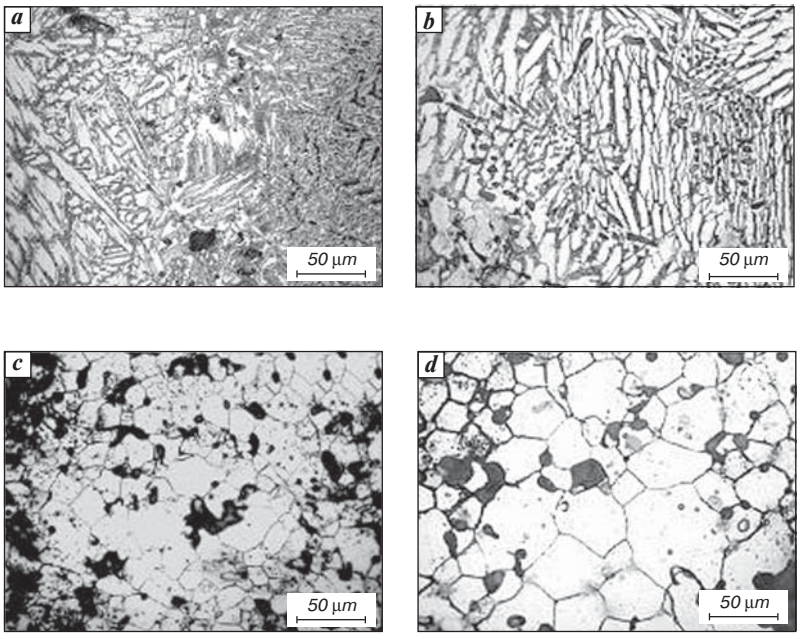

Fig. 3. Microstructure of the surface layer of TiNbTa (*a*, *c*) and TiNbZr (*b*, *d*) alloys after sintering at a temperature of 1873 K under vacuum of 1.33 Pa (*a*, *b*) and $1.33 \cdot 10^{-2}$ Pa (*c*, *d*)

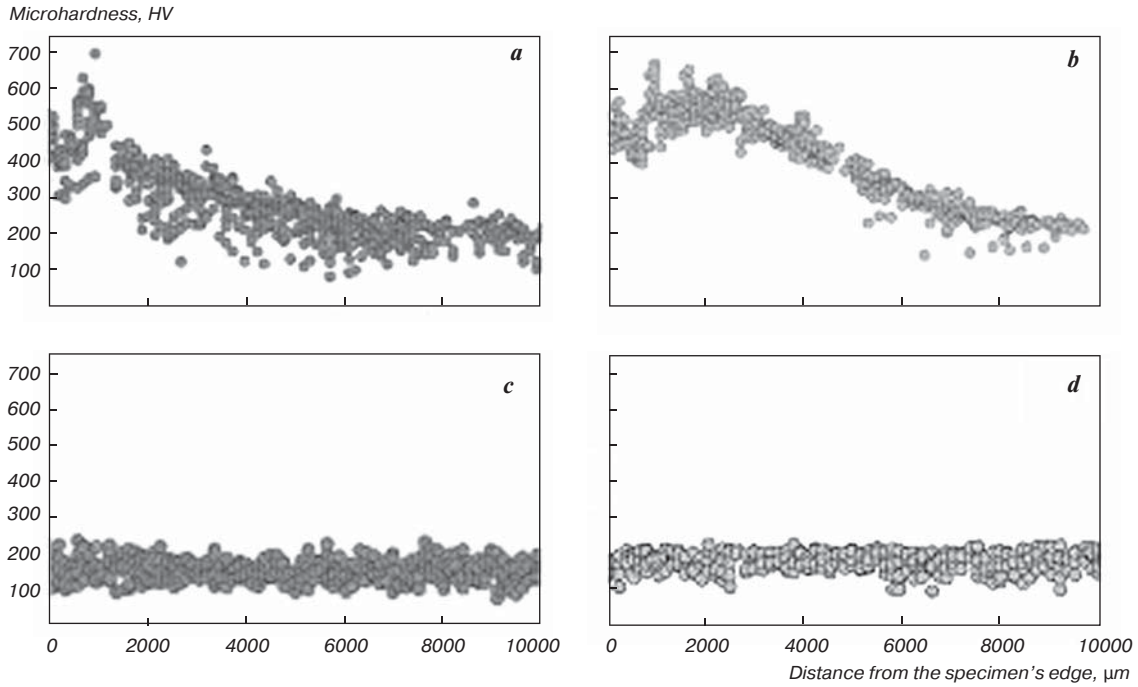

Fig. 4. The microhardness dependence of TiNbTa (*a*, *c*) and TiNbZr (*b*, *d*) specimens upon the distance from the layer's surface after sintering the alloys at a temperature of 1873 K vacuum of 1.33 Pa (*a*, *b*) and $1.33 \cdot 10^{-2}$ Pa (*c*, *d*)

Table 2

O, N and H content in TiNbTa and TiNbZr alloys sintered under different vacuum

Alloy	Sampling point	Vacuum, Pa	wt.%		
			O	N	H
TiNbTa	Surface	1.33	1.73	0.09	–
	Center		0.24	0.07	0.05
	Surface	$1.33 \cdot 10^{-2}$	0.23	0.09	–
	Center		0.22	0.10	0.02
TiNbZr	Surface	1.33	1.40	0.11	–
	Center		0.24	0.10	0.07
	Surface	$1.33 \cdot 10^{-2}$	0.22	0.01	–
	Center		0.22	0.03	0.03

In the TiNbTa and TiNbZr alloys sintered at 1873 K in vacuum of $1.33 \cdot 10^{-2}$ Pa an asymmetry of diffraction peaks is observed, which is especially noticeable at large angles 2θ (Fig. 5). Most likely, this is connected with presence of several solid solutions with an A2-type structure (the BCC lattice). The spectra of alloys have been satisfactorily described by two β-phases with different lattice spacing. The phase analysis results are given in Table 3.

It is possible that presence of two β-phases in the structure is caused by spinodal rupture which takes place in the Ti – Nb – Ta, Ti – Nb – Zr system. As indicated in [26], a tweed structure may be observed in a double alloy Ti – 35 at.% Nb (Ti – 51.1 wt.% Nb) after hardening and ageing at a temperature of 350 °C for 4 days, which may be a sign of spinodal decay of β-titanium. Koul M. K. and

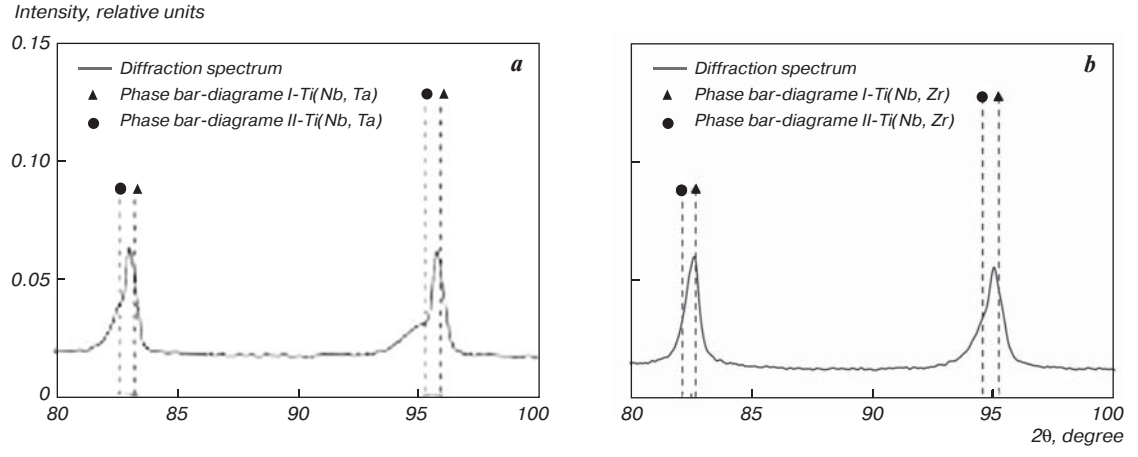

Fig. 5. Fragment of a difractogram of TiNbTa (*a*) and TiNbZr (*b*) alloys after pressing and sintering at 1873 K

Breedis J. F. in [27] point out that alloy Ti – 50 at.% Nb (Ti – 66 wt.% Nb) after hardening and ageing at a temperature of 450 °C during 30 day, most likely consists of two β-phases. According to the data in [28], it is noted that decomposition of β-phase into two by spinodal mechanism is possible in a cast four-component alloy Ti – 35Nb – 7Zr – 5Ta (wt.%). However, all these theses require to be defined more accurately since the observed β + β′ tweed structure doesn't give any additional reflections on its study by transmission electron microscopy, as it is presented in [26].

Table 3

The TiNbTa andTiNbZr phase content after pressing and sintering at 1873 K

Alloy	Phase	Vol. %	Periods, nm
TiNbTa	I-Ti(Nb,Ta) (type A2)	65	a = 0.3281
	II- Ti(Nb,Ta) (type A2)	35	a = 0.3299
TiNbZr	I-Ti(Nb,Zr) (type A2)	70	a = 0.3301
	II- Ti(Nb,Zr) (type A2)	30	a = 0.3319

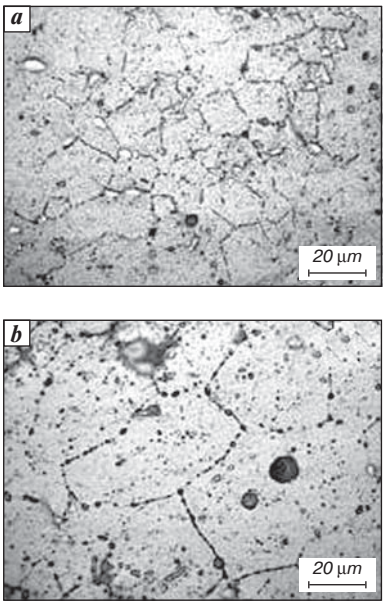

Fig. 6. The microstructure of TiNbTa (*a*) and TiNbZr (*b*) alloys after HIP

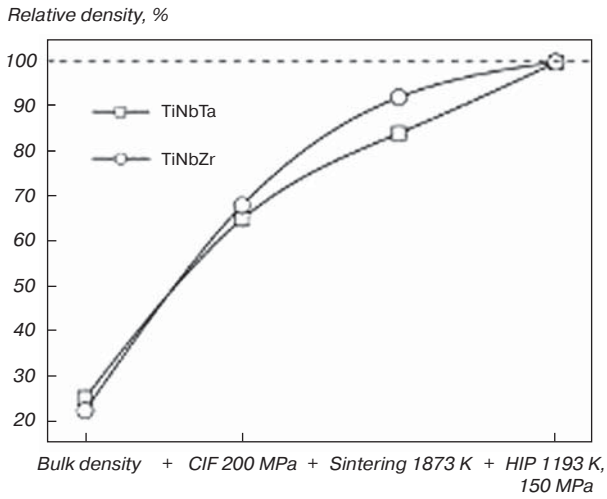

Fig. 7. Density of TiNbTa and TiNbZr alloys at various process stages

In that way, blanks with diameter of ~36 mm, length of 200 mm, weight of about 1100 g each have been produced by a technology of cold isostatic forming (CIF) the powders of TiNbTa and TiNbZr alloys under pressure of 200 MPa and sintering at a temperature of 1873 K in $1.33 \cdot 10^{-2}$ PA vacuum. Compact material has had porosity at levels of 16 and 8% for TiNbTa and TiNbZr, respectively.

Further porosity lessening of the blanks is possible by deformation only. In the context of the present paper, hot isostatic pressing (HIP) of sintered materials has been fulfilled. The HIP mode has been chosen according to the data of [29]. As a result, the porosity has been decreased until 1% for each alloy. The content of gas impurities relative to the sintered state didn't change. Microstructures of the specimens are shown in Fig. 6.

The main aim of consolidation is to transfer the powdered body with definite bulk density into a dense, compact blank. In the present paper it is demonstrated that density of TiNbTa and TiNbZr alloys is increasing on each processing stage and is approaching after HIP operation to the theoretical one (Fig. 7).

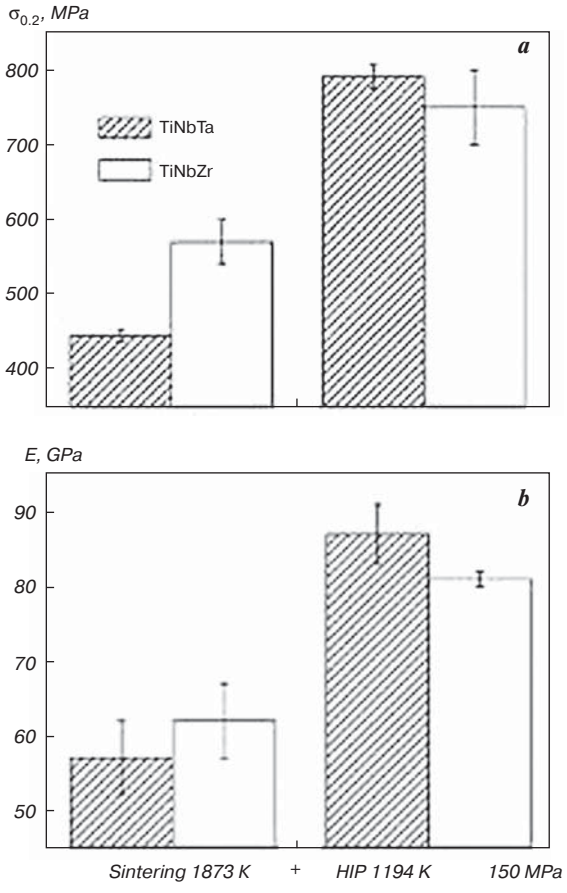

Fig. 8. The yield stress (*a*) and the Young's modulus (*b*) of TiNbTa and TiNbZr alloys in the sintered state and after HIP

Below are demonstrated the results of mechanical test of TiNbTa and TiNbZr alloys in the sintered state and after HIP (Fig. 8).

Analysis of the data, depicted in Fig. 7 and 8, shows that compacting and sintering operations of hydride-calcium powders of TiNbTa and TiNbZr alloys permits to obtain the blanks in a porosity state, and at the same time their porosity can be adjusted within define limits by changing the compacting and sintering modes. Mechanical strength ($\sigma_{0.2}$) and the Young's modulus of the porous blanks are comparable with characteristics of the cast intermetallic compound TiNi (Technical Requirments 1-809-253-80), applied as implant.

The HIP treatment of the porous blanks allows obtaining practically porousless TiNbTa and TiNbZr alloys with mechanical strength within the range of $\sigma_{0.2}$ ~750–800 MPa and the Young's modulus of ~80–90 GPa. After HIP the samples of TiNbTa and TiNbZr demonstrates close strength (Fig. 8, *a*). At the same time, an elastic modulus of TiNbTa alloy (Fig. 8, *b*) is rather higher than that of TiNbZr (87 ± 4 against 81 ± 1 GPa).

Conclusions

The executed work allows to make the following conclusions:

1. The powder technology under elaboration (hydrid-calcium synthesis + consolidation) permits to obtain blanks of TiNbTa and TiNbZr alloys both with regulated porosity and in practically porousless state.

2. It is shown that calcium hydride powders of TiNbTa and TiNbZr alloys distinguish themselves by good compactability according to a single-action compacting scheme as well as the CIF method. At the same pressure, CIF allows to obtain more dense and strong compacts.

3. The optimal temperature of sintering for the alloys under investigation has been determined as 1873 K by the trial sintering method. It is shown that even at a temperature of 1923 K the TiNbZr alloy sintering is possible.

4. Influence of the vacuum degree in the sintering process on quality of the finished blanks is described. If sintering (1873 K) takes place in low vacuum (~1.33 Pa), then the surface gas-filled layer is forming with heightened microhardness and the structure different from that of the main metal. Given such conditions of the experiment, the depth of this layer has amounted to ~8 mm. Sintering in high vacuum not worse than $1.33 \cdot 10^{-2}$ Pa is optimal and allows to obtain material with equal microhardness both on the surface and in the center of the blank and with uniform grain structure.

5. It is determined that sintering the TiNbTa and TiNbZr compacts with relative density of 65–68% at 1873 K leads to obtaining the material with a residual porosity of 16 and 8%, correspondingly. The porosity may be reduced practically to zero by further heat-strain treatment. For example, the porosity has been brought to 1% by HIP of the sintered blanks at 1193 K under pressure of 150 MPa.

6. The yield stress and modulus of elongation for TiNbTa and TiNbZr alloys in the states after sintering and HIF have been determined according to the scheme of uniaxial tension at room temperature. If the porosity is presented (the sintered state), the specimens demonstrates relatively low yield stress and the Young's modulus: $\sigma_{0.2} = 444 \pm 7$ MPa, $E = 57 \pm 5$ GPa for TiNbTa alloy and $\sigma_{0.2} = 570 \pm 29$ MPa, $E = 62 \pm 5$ GPa for TiNbZr alloy. In a practically porousless state (1% of pores), the strength and the Young's modulus of material demonstrate a regular growth: $\sigma_{0.2} = 791 \pm 16$ MPa, $E = 87 \pm 4$ GPa for TiNbTa alloy and $\sigma_{0.2} = 750 \pm 50$ MPa, $E = 81 \pm 1$ GPa for TiNbZr alloy.

The work was financially supported by the Russian Foundation for Basic Research (Project No. 16-43-710688 p_a). Determination of hydrogen content is performed within the framework of the State task No. 007-00129-18-00.

References

1. Niinomi M. Recent research and development in titanium alloys for biomedical applications and healthcare goods. *Science and Technology of Advanced Materials*. 2003. Vol. 4. pp. 445–454.

2. Balazic M., Kopac J., Jackson M. J., Ahmed W. Review: titanium and titanium alloy applications in medicine. *International Journal of Nano and Biomaterials*. 2007. Vol. 1, No. 1. pp. 3–34.

3. Brailovski V., Prokoshkin S., Gauthier M., Inaekyan K., Dubinskiy S., Petrzhik M., Filonov M. Bulk and porous metastable beta Ti – Nb – Zr(Ta) alloys for biomedical applications. *Materials Science and Engineering: C*. 2011. Vol. 31. pp. 643–657.

4. Ahmed T., Rack H. J. Low modulus biocompatible titanium base alloys for medical devices: Pat. 5871595 (USA). 1999.

5. Eisenbarth E., Velten D., Müller M., Thull R., Breme J. Biocompatibility of β-stabilizing elements of titanium alloys. Biomaterials. 2004. Vol. 25. pp. 5705–5713.

6. Kuroda D., Niinomi M., Morinaga M., Kato Y., Yashiro T. Design and mechanical properties of new β type titanium alloys for implant materials. *Materials Science and Engineering: A*. 1998. Vol. 243. pp. 244–249.

7. Matsuno H., Yokoyama A., Watari F., Uo M., Kawasaki T. Biocompatibility and osteogenesis of refractory metal implants, titanium, hafnium, niobium, tantalum and rhenium. *Biomaterials*. 2001. Vol. 22. pp. 1253–1262.

8. Sun J., Yao Q., Xing H., Guo W.Y. Elastic properties of β, α″ and ω metastable phases in Ti–Nb alloy from first-principles. *Journal of Physics: Condensed Matter*. 2007. Vol. 19. No. 48. pp. 1–8.

9. Ikehata H., Nagasako N., Furuta T., Fukumoto A., Miwa K., Saito T. First-principles calculations for development of low elastic modulus Ti alloys. *Physical Review B*. 2004. Vol. 70. pp. 174113-1–174113-8.

10. Gutiérrez Moreno J. J., Bönisch M., Panagiotopoulos N. T., Calin M., Papageorgiou D. G., Gebert A., Eckert J., Evangelakis G. A., Lekka Ch. E. Ab-initio and experimental

study of phase stability of Ti – Nb alloys. *Journal of Alloys and Compounds*. 2017. Vol. 696. pp. 481–489.

11. Gasik M. M., Yu H. Phase Equilibria and Thermal Behaviour of Biomedical Ti – Nb – Zr Alloy. *17th Plansee Seminar 2009 — International Conference on High Performance P/M Materials (25–29 May 2009) : proceedings and seminar impressions*. Reutte, 2009. Vol. 1. pp. 29/1–29/7.

12. Na L., Warnes W. H. Estimation of the Nb – Ti – Ta Phase Diagram. *IEEE Transactions on Applied Superconductivity*. 2001. Vol. 11. No. 1. pp. 3800–3803.

13. Collings E. W. Applied Superconductivity, Metallurgy, and Physics of Titanium Alloys: Their Metallurgical, Physical, and Magnetic-Mixed-State Properties. Springer Science & Business Media, 2013. 834 p.

14. Souza S. A., Manicardi R. B., Ferrandini P. L., Afonso C. R. M., Ramirez A. J., Caram R. Effect of the addition of Ta on microstructure and properties of Ti – Nb alloys. *Journal of Alloys and Compounds*. 2010. Vol. 504. pp. 330–340.

15. Konopatskii A. S., Zhukova Yu. S., Dubinskii S. M., Korobkova A. A., Filonov M. R., Prokoshkin S. D. Microstructure of Superplastic Alloys Based on Ti–Nb for medical purposes. *Metallurgist*. 2016. Vol. 60, Nos. 1–2. pp. 223–228.

16. Konopatsky A., Zhukova Yu., Dubinsky S., Filonov M., Prokoshkin S. Production of Novel Superelastic Biocompatible Ti – Nb-based Alloys for Medical Application. *ESOMAT 2015 — 10th European Symposium on Martensitic Transformations. MATEC Web of Conferences (14–18 September, 2015) : proceedings*. Belgium: EDP Sciences. 2015. Vol. 33. p. 06003-p.1-06003-p.5.

17. Martins D. Q., Os rio W. R., Souza M. E. P., Caram R., Garcia A. Effects of Zr content on microstructure and corrosion resistance of Ti – 30Nb – Zr casting alloys for biomedical applications. *Electrochimica Acta*. 2008. Vol. 53. pp. 2809–2817.

18. Kasimtsev A. V., Shuytsev A. V., Yudin S. N., Levinskyi Yu. V., Sviridova T. A., Alpatov A. V., Novosvetlova E. E. Hydrid-calcium synthesis of powders of Ti – Nb-based. *Metally*. 2017. No. 5. pp. 52–63.

19. Shelekhov E. V., Sviridova T. A. Programs for *X*-ray Analysis of Polycrystals. *Metal Science and Heat Treatment*. 2000. Vol. 42. No. 8. pp. 309–313.

20. Robertson I. M., Schaffer G. B. Review of densification of titanium based powder systems in press and sinter processing. *Powder Metallurgy*. 2010. Vol. 53. No. 2. pp. 146–162.

21. Kang S. J. L. Sintering: densification, grain growth and microstructure. Elsevier Butterworth-Heinemann, 2004. 265 p.

22. Eremenko V. N., Tretyachenko L. A. Triple titanium systems with transition metals of IV–VI groups. Kiev: Naukova Dumka, 1987. 232 p.

23. Zhukova Yu. S. Production and characterization of superelastic Ti – Nb – Ta, Ti – Nb – Zr alloys fro medical applications: thesis of inauguration of Dissertation ... of Candidate of Engineering Sciences. Moscow: MISiS, 2013. 23 p.

24. Liu Z., Welsch G. Effects of Oxygen and Heat Treatment on the Mechanical Properties of Alpha and Beta Titanium Alloys. *Metallurgical Transactions: A*. 1988. Vol. 19. pp. 527–542.

25. Malinov S., Zhecheva A., Sha W. Relation between the Microstructure and Properties of Commercial Titanium Alloys and the Parameters of Gas Nitriding. *Metal Science and Heat Treatment*. 2004. Vol. 46. Nos. 7–8. pp. 286–293.

26. Moffat D. L., Larbalestier D. C. The Competition between the Alpha and Omega Phases in Aged Ti – Nb Alloys. *Metallurgical Transactions: A*. 1988. Vol. 19. pp. 1687–1694.

27. Koul M. K., Breedis J. F. Phase Transformations in Beta Isomorphous Titanium Alloys. *Acta Metallurgica*. 1970. Vol. 18. pp. 579–588.

28. Afonso C. R. M., Ferrandini P. L., Ramirez A. J., Caram R. High resolution transmission electron microscopy study of the hardening mechanism through phase separation in a β – Ti –35Nb – 7Zr – 5Ta alloy for implant applications. *Acta Biomaterialia*. 2010. Vol. 6. pp. 1625–1629.

29. Atkinson H. V., Davies S. Fundamental Aspects of Hot Isostatic Pressing: An Overview. *Metallurgical and Materials Transactions: A*. 2000. Vol. 31. pp. 2981–3000.

NFM